LAWRENCE
LIVERMORE
NATIONAL
LABORATORY

LLNL-JRNL-811903

Tropospheric Temperature

J. R. Christy, C. A. Mears, S. Po-Chedley, L. Haimberger

June 23, 2020

Bulletin of the American Meteorological Society

Disclaimer

Tropospheric temperature—J.R. Christy, C. A. Mears, S. Po-Chedley, and L. Haimberger

The 2019 global lower tropospheric temperature (LTT), which encompasses the atmosphere from the surface to ~10 km, ranked second warmest in seven datasets and first or third in the remaining two (Fig. 2.7). These records extend back to 1958 using radiosonde (balloon-borne instrumentation) data and one reanalysis dataset (JRA55), which demonstrate reasonable agreement with the 40+ year satellite record (since late 1978) and two other reanalysis datasets (since 1979 and 1980, ERA5 and MERRA2, respectively). A weak El Niño contributed to increased global temperatures as 2019 values were +0.44° to +0.68°C higher than the 1981–2010 average (depending on the dataset), being just slightly cooler (~0.07°C on average) than the record warm year of 2016. At least four of the five globally complete datasets (ERA5, MERRA2, JRA55, RSS, UAH) recorded each of the four months—June, September, November, and December—as experiencing their warmest monthly global LTT.

The warming rate of the global troposphere since 1958, as the median of available datasets, is +0.18 (range +0.16 to +0.20) °C decade^{-1}. The median warming rate since 1979 is also +0.18 (range +0.13 to +0.21) °C decade^{-1}, which includes records derived from microwave satellite measurements (Table 2.3). Taking into consideration the temporary cooling due to volcanic aerosols caused by eruptions in 1982 and 1991, as well as the El Niño/La Niña cycle, there remains a global warming trend since 1979 of +0.12 ± 0.04°C decade^{-1} unexplained by these ephemeral, natural phenomena (Christy and McNider 2017, updated and calculated using ERA5, RSS, and UAH datasets).

The spatial details of the departures of LTT from the 1981–2010 mean are depicted in Plate 2.1e as provided by the European Centre for Medium-Range Forecasts Reanalysis version 5 (ERA5). Above-average anomalies dominate the 2019 ERA5 map with negative regions occupying only 8.1% of the global surface area, including much of North America, a portion of South Asia, and midlatitude regions of the southern oceans. These below-average LTTs comprise the third-smallest such area after 2016 and 2017.

Much higher-than-average temperatures included several regions that experienced record high temperatures relative to this 41-year period of observations. Alaska, Greenland, central Europe, and southern Africa were especially warm. The broad warmth of the tropical belt is a typical signature of an El Niño year.

The warming trend may be depicted in a geographical context by determining the year in which the extreme high (and low) annual values at each grid point occurred, then summing those areally-weighted grids by year. If all regions of Earth experienced a monotonically increasing temperature, then each new year would see 100% of the global area achieving a record high temperature; however, if the global trend were zero over the 41-year period of record but characterized by random inter-annual variability, each year would experience, on average, an area of 2.4% of record high (or low) temperatures. With our climate system characterized by both an increasing trend and inter-annual variations since 1979, the area in 2019 of record high temperatures was 15.6% (calculated as the average of ERA5, RSS, and UAH). The stippling in Plate 2.1e identifies these grids (see also Fig. A2.6). Two years with major El Niño events, 1998 and 2016, recorded areal extents for the highest temperatures of 16.9% and 20.1%, respectively (no repeated records). Since 1979, the year with the largest coverage of record low annual-average temperatures was 1985 with 19.8% due in part to a concurrent La Niña event.

Global and tropical trends are listed in Table 2.3. When examining the time series of these three methods (radiosondes, satellites, reanalyses), the radiosondes display an increasing trend over the past 10 years relative to the other methods (see trend values in column Global LTT 1979 and Fig. A2.7) This may be

related to a change in software installed after 2009 in many stations to improve the tropospheric humidity and temperature values (Christy et al. 2018).

The tropical (20°N–20°S) tropospheric temperature (TTT, surface to ~15 km) variations and trends are similar to those of the global values. The median TTT trends from the available datasets since 1958 and 1979 are both +0.16°C decade^{-1} with ranges of +0.15 to +0.19 and +0.13 to +0.23°C decade^{-1}, respectively (Table A2.1). This layer in the tropics is a key area of interest due to its expected significant response to forcing, including that of increasing greenhouse gas concentrations (McKitrick and Christy 2018; see Fig. A2.8).

Radiosondes provide coverage wherever the stations exist. Considerable areas of the globe are thus not sampled, and this can lead to a misrepresentation of the global average. Satellites essentially observe the entire Earth each day, providing excellent geographic coverage, but whose radiances provide bulk-layer atmospheric measurements only. There are some key adjustments that are required too, and the methods adopted by different teams lead to the range in the results (Haimberger et al. 2012; Po-Chedley et al. 2015; Mears and Wentz 2016; see also Figs. A2.7 and A2.9). Full input reanalyses use essentially all available data, including radiosonde and satellite, ingested into a continuously updated global circulation model, thus providing full geographic and vertical coverage. Given the many differences in how the reanalyses are constructed from center to center, the consistency among their 41-year trends is encouraging.

References

Christy, J. R., and R. T. McNider, 2017: Satellite bulk tropospheric temperatures as a metric for climate sensitivity. *Asia-Pacific J. Atmos. Sci.*, **53**, 511–518, https://doi.org/10.1007/s13143-017-0070-z.

— , S. Po-Chedley, C. Mears, and L. Haimberger, 2019: Lower tropospheric temperature [in "State of the Climate in 2018"]. *Bull. Amer. Meteor. Soc.*, **100** (8), S16–S17, https://doi.org/10.1175/2019BAMSStateoftheClimate.1.

Haimberger, L., C. Tavolato, and S. Sperka, 2012: Homogenization of the Global Radiosonde Temperature dataset through combined comparison with re- analysis background series and neighboring stations. *J. Climate*, **25**, 8108– 8131, https://doi.org/10.1175/JCLI-D-11-00668.1.

McKitrick, R., and J. R. Christy, 2018: A test of the tropical 200- to 300-hPa warming rate in climate models. *Earth Space Sci.*, **5**, 529–536, https://doi. org/10.1029/2018ea000401.

Mears, C. A. and F. J. Wentz, 2016: Sensitivity of satellite-derived tropospheric tem- perature trends to the diurnal cycle adjustment. *J. Climate*, **29**, 3629–3646, https://doi.org/10.1175/JCLI-D-15-0744.1.

Acknowledgements

Work performed by Stephen Po-Chedley at LLNL was performed under the auspices of the U.S. Department of Energy under Contract DE-AC52-07NA27344 and under LDRD 18-ERD-054. This work is published under LLNL-JRNL-811903.

Figures

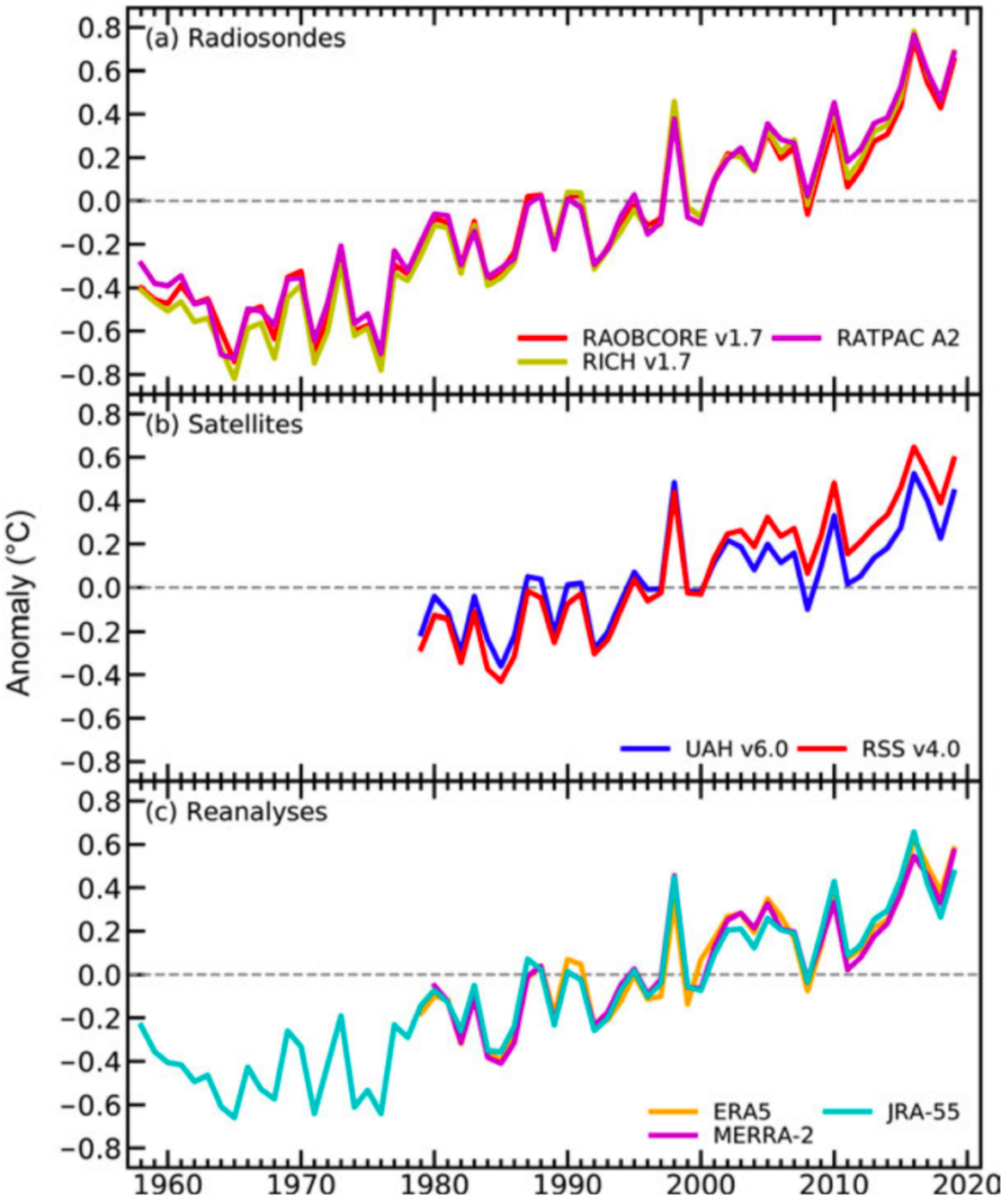

Fig. 2.7. Time series of global annual temperature anomalies (°C) for the lower troposphere from (a) radiosondes, (b) satellite microwave emissions, and (c) reanalyses.

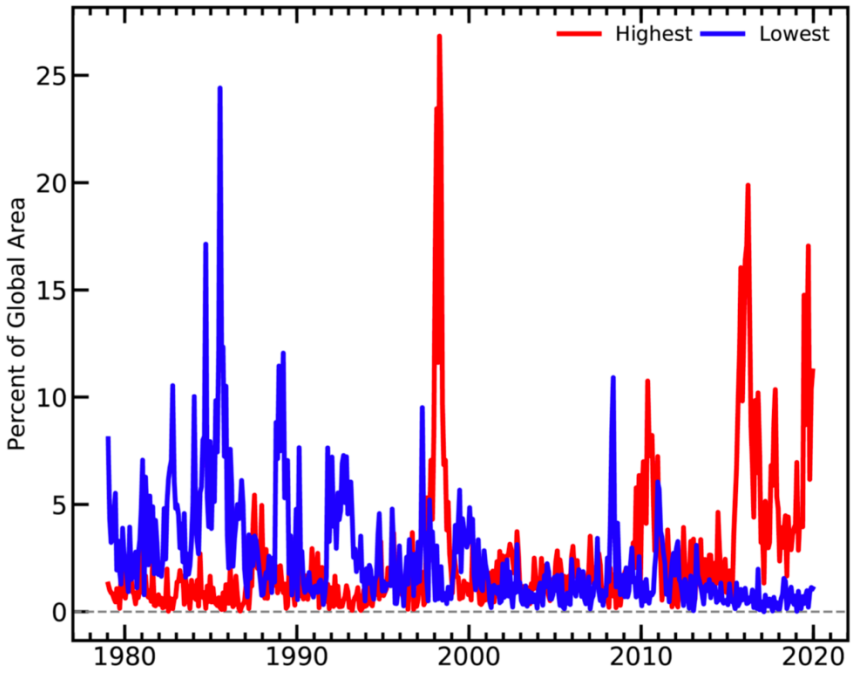

Fig. A2.6. Average area of highest (red) (blue) and lowest temperatures by month for the 41 years of observations in ERA5, RSS, and UAH datasets. This is an update of the figure from SotC 2018 (Christy et. al. 2019).

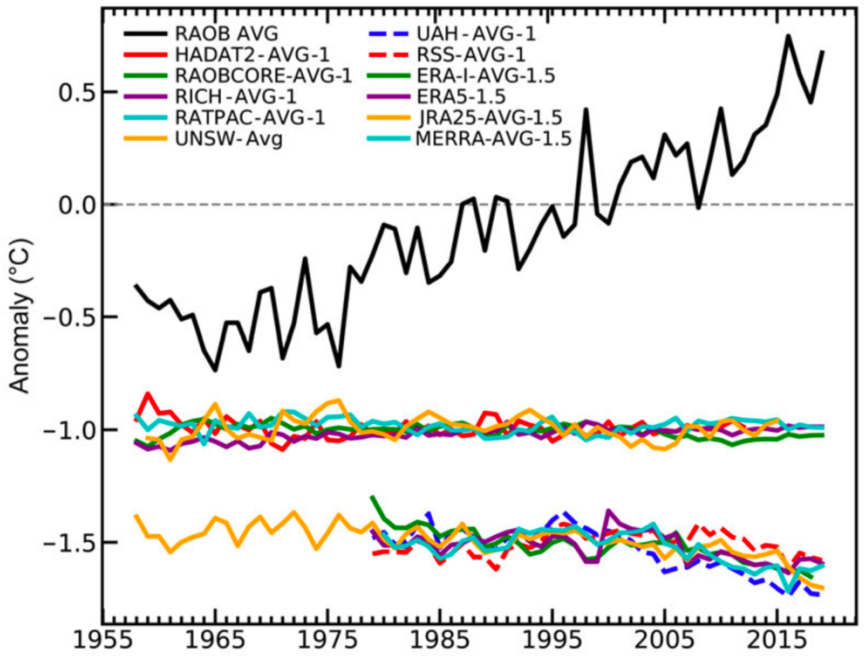

Fig. A2.7. (Top) Time series of annual anomalies of global lower tropospheric temperature (°C)from radiosonde datasets only. (Middle) Differences of individual radiosonde datasets (at –1.0°C axis) versus the radiosonde average. (Bottom) Differences relative to the radiosonde average (top) for satellite and reanalyses (at –1.5°C axis). As noted in the text, those datasets that are not exclusively radiosondes (bottom) show decreasing values after 2009 possibly related to spurious warming in the radiosondes as a consequence of a change in the software processing system at many of the stations.

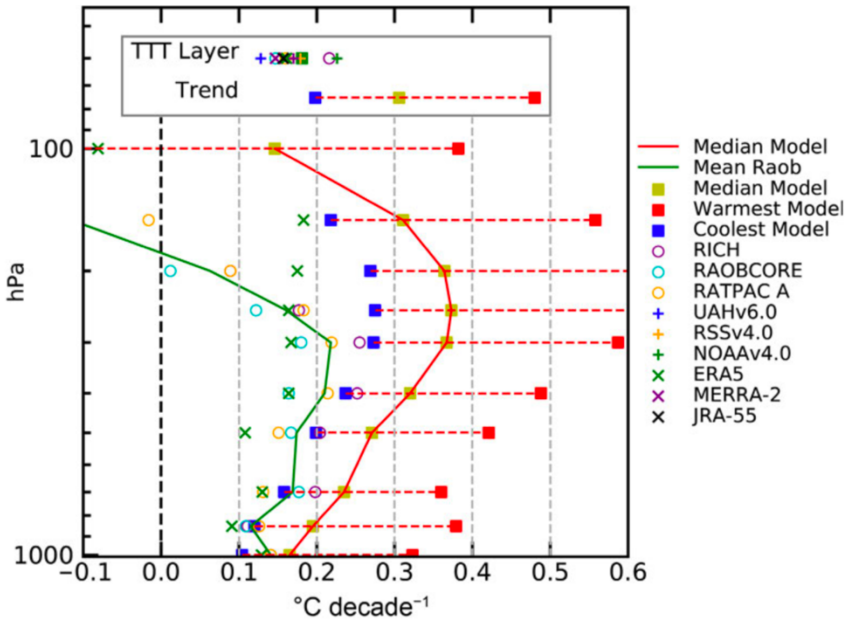

Fig. A2.8. Update of tropical temperature (TTT) trend comparisons (1979–2019) from SotC 2016 (Christy 2017) between observational datasets and the Climate Model Intercomparison Project version 6 (CMIP-6). The trend values for each pressure level are shown from 1000 to 100 hPa with central values represented by the green (mean radiosondes) and red (median model) lines. The upper box provides the trends for the average of the bulk atmospheric layer TTT as described in the text. The model time series are constructed with historical forcings from 1850 to 2014 and after 2014 with forcing scenario ssp245. The 30 CMIP-6 models used are ACCESS-CM2, ACCESS-ESM1-5, AWI-CM-1-1-MR, BCC-CSM2-MR, CanESM5 (warmest), CanESM5-OE, CESM2, CESM2-WACCM, CNRM-CM6-1, CNRM-ESM2, EC-EARTH3, EC-EARTH3-VEG, FGOALS, FIO, GFDL-CM4, GFDL-ESM, GISS-E2-1-G, HadGEM, INM-CM4-8, INM-CM5-0, IPSL-CM6A-LR, MCM-UA, MIROC6, MIROC6-2L MPI-ESM1-2-HR, MPI-ESM1-2-LR, MRI-ESM2-0 (coolest), NESM, NorESM2-LM, and UKESM1-0-LL.

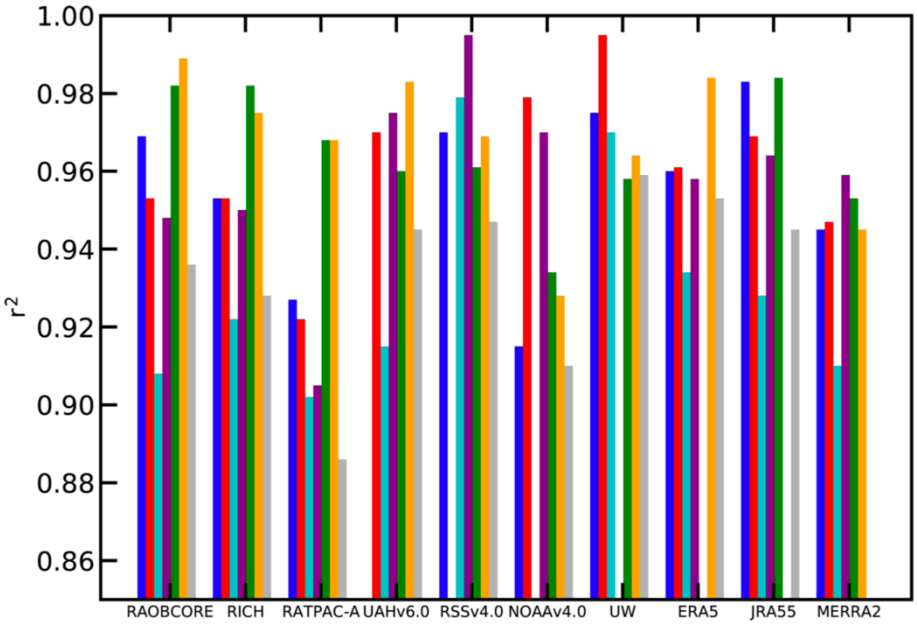

Fig. A2.9. Paired intercomparisons of the datasets utilized here for the tropical TTT metric, calculating the extent to which the identified paired datasets agree in terms of common variance (r^2).

Tables

Table 2.3. Estimates of lower tropospheric temperature (LTT) and tropical tropospheric temperature (TTT) decadal trends (°C decade^{-1}) beginning in 1958 and 1979 from the available datasets.

Area		Global	Global	Tropical	Tropical
Layer		LTT	LTT	TTT	TTT
Start Year		1958	1979	1958	1979
Radiosonde	NOAA/RATPACvA2	+0.18	+0.21	+0.16	+0.16
	RAOBCOREv1.7	+0.18	+0.19	+0.15	+0.15
	RICHv1.7	+0.20	+0.21	+0.19	+0.22
Satellite	RSSv4.0	—	+0.21	—	+0.18
	UAHv6.0	—	+0.13[1]	—	+0.13
	NOAA/STARv4.1	—	—	—	+0.23
	UWv1.0	—	—	—	+0.17
Reanalyses	ERA5	—	+0.17	—	+0.16
	JRA-55	+0.16	+0.16	+0.16	+0.15
	NASA/MERRA-2[2]	—	+0.17	—	+0.16
Median		**+0.18**	**+0.18**	**+0.16**	**+0.16**

[1]The UAH LTT weighting function is slightly different in order to reduce the impact of surface emissions and enhance the tropospheric signal, resulting in a global trend value typically cooler by 0.01°C decade^{-1} relative to the standard LTT weighting function.

[2]NASA/MERRA-2 begins in 1980.

Table A2.1. Comparison of decadal trend values (°C decade^{-1}) between observations and CMIP-6 climate model simulations. (See Fig. A2.8)

Area		Global	Global	Tropical	Tropical
Layer		LTT	LTT	TTT	TTT
Start year		1958	1979	1958	1979
Median	Observations	+0.18	+0.18	+0.16	+0.16
Median	CMIP6 (30 models)	+0.20	+0.29	+0.22	+0.32